Numerical studies of optical forces from adiabatic rapid passage

Daniel Stack,[1] John Elgin,[1] Petr M. Anisimov,[2] and Harold Metcalf[1]
[1]*Physics and Astronomy, Stony Brook University, Stony Brook, New York 11794-3800, USA*
[2]*Hearne Institute for Theoretical Physics and Department of Physics and Astronomy, Louisiana State University, Baton Rouge, Louisiana 70803, USA*
(Received 24 May 2011; published 25 July 2011)

We present a numerical study of the properties of optical forces on moving atoms derived from purely stimulated processes produced by multiple adiabatic rapid-passage sequences. The optical Bloch equations are solved for a carefully timed sequence of frequency-swept pulses that can produce a force much larger than the ordinary radiative force. We describe the effects of the sweep range, peak intensity, sweep direction, number of pulses, atomic velocity, and spontaneous emission. Since the momentum of thermal atoms is much larger than that transferred by a single absorption-stimulated emission cycle, multiple repetitions are needed to make a significant velocity change.

DOI: 10.1103/PhysRevA.84.013420 PACS number(s): 37.10.De, 37.10.Vz

I. INTRODUCTION

The notion of optical forces, derived from linear momentum conservation during atomic absorption of light, dates back to the 19th century. The advent of lasers has enabled laser cooling, optical lattices, atom optics and interferometry, quantum information studies, BEC, and a host of other topics [1]. When an atom of mass M absorbs light, its energy $\hbar\omega_\ell$ goes mostly into the excitation of the atom, its angular momentum $\hbar$ goes into the orbital motion of the electrons, but its linear momentum $\hbar\omega_\ell/c \equiv \hbar k$ can go only into the overall translational motion of the atom. The atomic velocity changes by $\hbar k/M \sim$ few cm/s. The magnitude of the resulting force is limited by how quickly this momentum exchange can be repeated and thus by the rate of the atom's return to the ground state. Return via spontaneous emission limits the force to $F_{sp} = \hbar k\gamma/2$ where $\tau \equiv 1/\gamma$ is the natural lifetime of the excited state.

By contrast, stimulated emission can bring atoms to their ground state much faster, but the stimulated light must have a $\mathbf{k}$ vector different from that of the exciting light or the net momentum transfer, thus, the force, will vanish. An absorption-stimulated emission sequence from counterpropagating beams leads to a very large force, but this force alternates sign on the wavelength scale and is therefore of limited utility.

A series of properly tailored pulses designed to cause absorption-stimulated emission cycles can produce a strong unidirectional force. An efficient pulse pair would leave the atom in its excited state $|e\rangle$ after the first pulse and its ground state $|g\rangle$ after the second pulse. This can be achieved with "π pulses" [2,3], but such an approach is not very robust against variations in experimental conditions. By contrast, optical adiabatic rapid passage (ARP) [4] is a coherent control process that enables inversion and the concomitant momentum exchange in a way that is more resistant to experimental parameter variations. This has been demonstrated in our earlier work where we explored optical forces based on ARP numerically, analytically, and experimentally [5–8].

In this paper, we extend our previous Bloch vector description of a single ARP process that was based on an absorption-stimulated emission cycle to the numerical solution of the optical Bloch equations. This allows us to calculate the effect of multiple ARP cycles using increasing, decreasing, or alternating frequency sweeps of consecutive pulses. We also include the unavoidable phase shifts and drifts that derive from atomic motion and/or experimental limitations.

Moreover, our present model also allows us to investigate the velocity dependence of the ARP force and to define its range of velocities, a parameter that is very important for use in laser cooling. We can also introduce spontaneous decay into the optical Bloch equations. This leads to the expected reduction of the optical force that we attribute to the decreasing length of the Bloch vector, but it also shows unexpected results such as a directional asymmetry in the velocity dependence of the force.

Following a brief introduction to the ARP process in Sec. II, we discuss the force on stationary atoms and then the velocity dependence of the force in Secs. III A and III B, all in the absence of spontaneous emission. In Sec. IV, we present the effects of spontaneous emission on the velocity dependence of the force with some interesting consequences. Finally, in Sec. V, we discuss the velocity capture range of the force, and conclude in Sec. VI.

II. ADIABATIC RAPID PASSAGE

ARP has long been known in the magnetic resonance community as a way to invert the population of a two-level system by sweeping the frequency of the applied field through resonance. This process is best visualized though the path of the well-known Bloch vector $\mathbf{R} = [u, v, w]$ on the Bloch sphere (see Refs. [2,3,9]). In this view, the south pole $\mathbf{R} = [0,0,-1]$ represents a ground state $|g\rangle$ and the north pole $\mathbf{R} = [0,0,1]$ represents an excited state $|e\rangle$.

The Schrödinger equation shows that the evolution of the Bloch vector is governed by an artificial "torque" vector $\mathbf{\Omega} \equiv [\Omega_r, \Omega_i, -\delta]$, according to $d\mathbf{R}/dt = \mathbf{\Omega} \times \mathbf{R}$ [2,3,9]. Here, $\Omega_{r,i}$ are the real and imaginary parts of the Rabi frequency (complex to denote phase) with slowly varying amplitude given by $\hbar\Omega(t) \equiv \langle g|e\mathcal{E}(t)\cdot\mathbf{r}\,|e\rangle$. Also, $\delta(t) \equiv \omega_\ell(t) - \omega_a$ is the detuning of the optical frequency $\omega_\ell(t)$ from the atomic frequency ω_a.

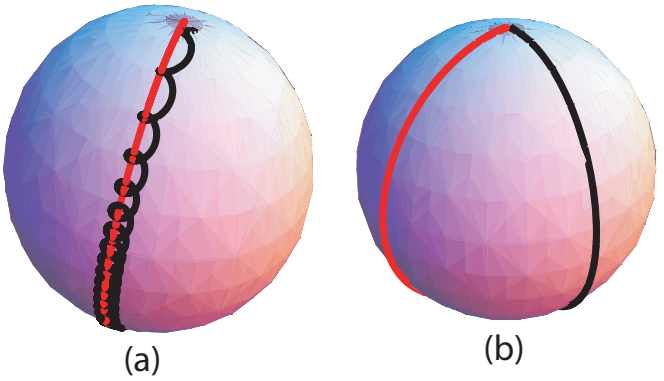

FIG. 1. (Color online) Plot of two trajectories (the north pole shown) of $\mathbf{R}(t)$ and $\mathbf{\Omega}(t)$. Part (a) has $\delta_0 = 30\,\omega_m$ and $\Omega_0 = 50\,\omega_m$ to show the usual ARP where $\mathbf{R}$ (black curve) makes many precession cycles and stays close to Ω (smooth red trace) during the sweep. Part (b) has $\delta_0 = 1.10\,\omega_m$ and $\Omega_0 = 1.61\,\omega_m$ to show the unusual case where the trajectory of $\mathbf{R}$ is a simple arc along a meridian that is $\sim 90^\circ$ away from the path of Ω (red trace on the left).

In the usual Bloch sphere picture of ARP, the torque vector $\mathbf{\Omega}$ begins near the south pole, nearly parallel to $\mathbf{R}$, and is slowly swept toward the north pole by changing δ from a large positive value to a large negative value over a range of $2\delta_0$, while the amplitude of the Rabi frequency increases to its maximum value Ω_0 at $\delta = 0$, followed by its decrease [6]. Although different pulse profiles have been considered [8], here we choose a sweep characterized by $\delta(t) = \delta_0 \cos(\omega_m t)$ and $\Omega(t) = \Omega_0 |\sin(\omega_m t)|$ that can start at $t = 0$ and last for time π/ω_m.

Traditionally, ARP is thought to be most robust when the parameters satisfy

$$\delta_0 \sim \Omega_0 \gg \omega_m \gg \gamma \tag{1}$$

so that the trajectory of $\mathbf{R}$ on the Bloch sphere tracks Ω in a nearby spiral path. Such a single pulse can transport $\mathbf{R}$ initially at $(0, 0, -1)$ toward the north pole as shown in Fig. 1(a), thus producing the atomic inversion. In this case, the parameters satisfy Eq. (1) so that the rapid precession of $\mathbf{R}$ about Ω keeps the angle between them quite small. Unlike the π-pulse method, this process is very robust against optical frequency and amplitude variations. Reversing the initial direction of Ω, or reversing the sweep direction, results in different paths for $\mathbf{R}$ but does not change the end points of its trajectory. Thus, if an atom starts near the north pole, such a frequency-swept pulse leaves it near the south pole.

We have shown in Ref. [5], however, that orbits similar to that of Fig. 1(b) are nearly as robust with parameters characterized by $\delta_0 \sim \Omega_0 \sim \omega_m \gg \gamma$ even though they are well outside the usual ARP domain associated with Eq. (1). Unlike the case for Fig. 1(a), $\mathbf{R}$ and $\mathbf{\Omega}$ are nearly orthogonal when they pass through the equatorial plane. The sweep of Fig. 1(b) is also adiabatic, although in a different sense, and is more suitable as a source for optical forces because it allows much faster absorption-stimulated emission cycles. This prediction from Ref. [5] has been experimentally corroborated [6].

The timing scheme for ARP-based absorption-stimulated emission cycles is illustrated in Fig. 2. A pulse of duration π/ω_m from one direction (e.g., from the left) is represented by the half-period sine wave in the upper trace, and its upward frequency sweep is represented by the curve in the lower trace. A second pulse, incident from the opposite direction (e.g., from the right), is represented by the second half-period sine wave, also with an upward frequency sweep. Then, there is a dead time of $2\pi/\omega_m$ for experimental reasons [6] as well as the theoretical reasons that will become obvious below, and the sequence is repeated. In this simple picture, the optical force from a pulse pair is $F_{\rm ARP} \equiv \hbar k \omega_m/\pi$ [10] and can be orders of magnitude larger than the ordinary radiative force F_{sp}.

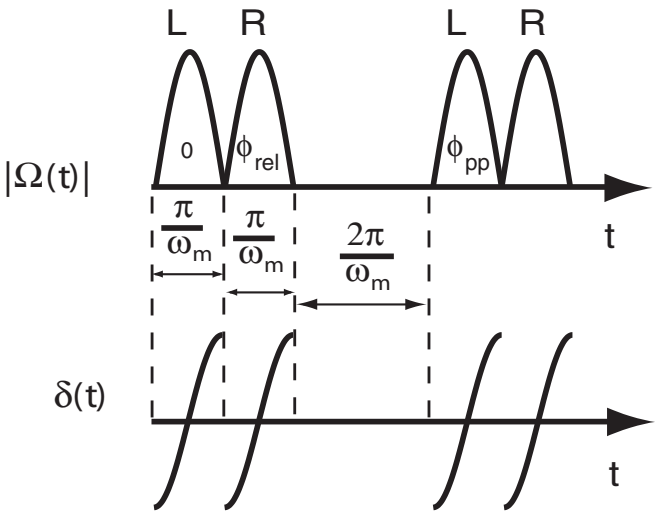

FIG. 2. The upper trace shows the Rabi frequency $\Omega(t)$ during the pulse pair followed by the dead time, and then the next pulse pair. The lower trace shows the frequency sweep $\delta(t)$, in this case both upward. (Figure adapted from Ref. [6].)

Our previous numerical calculations were based on the efficiency of exciting an atom to the north pole by a single pulse or returning an atom to the south pole by a pulse pair. Note that return to the south pole after a pulse pair means an exchange of $\sim 2\hbar k$ only if $\mathbf{R}$ went near the north pole after the first pulse. The figure of merit was the success rate of these processes, and we sought the range of sweep extrema δ_0 and Ω_0 that were most effective in doing so. By contrast, our use of the optical Bloch equations here enables us to calculate the optical force over multiple ARP sequences, and also to include the effects of Doppler shifts and spontaneous emission. We write these equations in the interaction picture as

$$\dot{\tilde{u}} = \Omega_i \tilde{w} - (\gamma/2)\tilde{u},$$
$$\dot{\tilde{v}} = -\Omega_r \tilde{w} - (\gamma/2)\tilde{v},$$
$$\dot{\tilde{w}} = \Omega_r \tilde{v} - \Omega_i \tilde{u} - \gamma(\tilde{w} + 1),$$

and

$$\Omega = \Omega_0 |\sin(\omega_m t)| \exp[i\alpha(t)]. \tag{2}$$

Here, the frequency detuning $\delta(t)$ is included in the complex phase $\alpha(t)$ as $-(\delta_0/\omega_m)|\sin(\omega_m t)|$ along with contributions that come from Doppler shifts $(\mathbf{k}\cdot\mathbf{v})t$ and unavoidable phase differences between pulses in a pair $\phi_{\rm rel}$, as well as between pairs ϕ_{pp}. We solve these equations numerically in Fortran-90 using the BIM subroutine [11].

III. ARP FORCE ON TWO-LEVEL ATOMS

A. ARP force on stationary atoms

In the absence of spontaneous emission, stationary atoms are described by the equations similar to those we used previously to study dependence of optical forces from single swept pulses [8]. However, phase differences between pulses $\phi_{\rm rel}$ and ϕ_{pp} caused by atomic motion and the jitter of the timing that starts each sequence, respectively, are unavoidable experimentally and their effects are discussed below.

To demonstrate the effects of phase, we choose to vary $\phi_{\rm rel}$ while holding $\phi_{pp} = 0$ and calculate the average optical force over the duration of the pulse sequence. Figure 3 shows maps of the optical force averaged over 12 pulse pairs calculated for various values of Ω_0 and δ_0 ranging over several times ω_m. These maps show that the optical force depends strongly on relative phase as well as on the sweep directions in the consecutive ARP pulses.

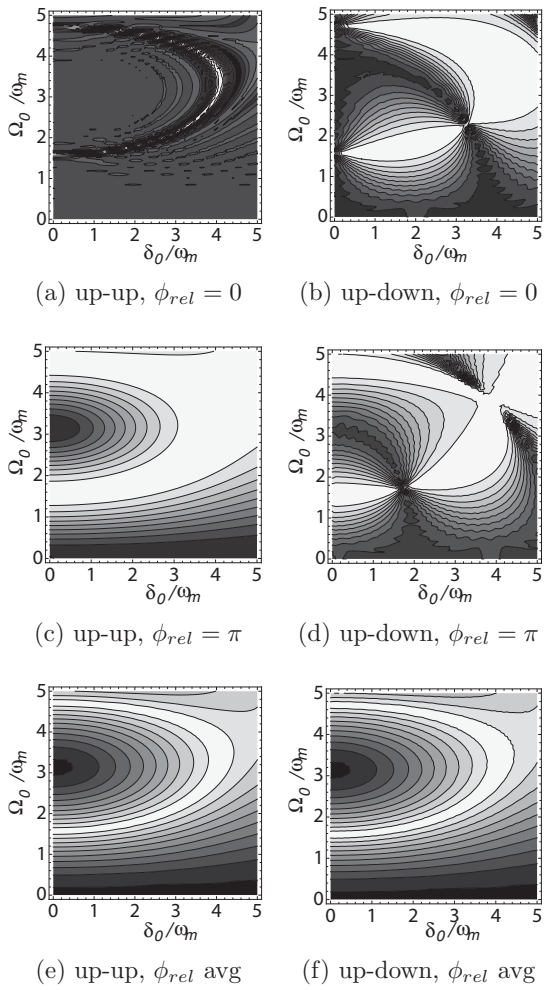

(a) up-up, $\phi_{rel} = 0$ (b) up-down, $\phi_{rel} = 0$

(c) up-up, $\phi_{rel} = \pi$ (d) up-down, $\phi_{rel} = \pi$

(e) up-up, ϕ_{rel} avg (f) up-down, ϕ_{rel} avg

FIG. 3. Contour plots of the average force calculated over a range of the experimental parameters Ω_0 and δ_0 scaled by ω_m. White regions represent areas with the greatest average force, approximately $F_{\rm ARP}/2$, and the darkest regions correspond to zero average force. The left column [parts (a), (c), and (e)] are for all sweeps upward, corresponding to the experiments of Ref. [6]. Part (a) shows the case for $\phi_{\rm rel} = 0$, part (c) shows the case for $\phi_{\rm rel} = \pi$, and part (e) shows the average over the region between 0 and π. The right-hand column shows the corresponding results for pulse pairs with up-down sweep sequences. We leave $\phi_{pp} = 0$ in all plots.

The "up-up" case (left-hand column) describes an ARP pulse pair with $\delta_0 > 0$ leading to the upward evolution of the torque vector on the Bloch sphere. It corresponds to our experiments using a retroreflected train of light pulses with appropriate delays that necessarily resulted in pulse pairs with the same upward or downward sweeps (see Ref. [6]). Figure 3(a) shows the average calculated force with $\phi_{\rm rel} = 0$. The strength of the ARP force is more sensitive to the values of Ω_0 and δ_0 than in Ref. [5] because those calculations were done for a single sweep and deviations from the ideal case accumulate with each successive sweep. Nevertheless, even after a very large number of sweeps, there is a very strong ARP force for parameter values that do not satisfy the traditional conditions given in Eq. (1) [5].

By contrast, the choice of $\phi_{\rm rel} = \pi$ is quite different [see Fig. 3(c)]. Here, each optical pulse has a π phase shift relative to its neighbors that clearly makes ARP much more robust against changes in Ω_0 or δ_0. This can be understood by examining the trajectories of **R** for sequential sweeps that show successive paths partially compensating for the errors produced by their predecessors.

The "up-down" case (right-hand column) corresponds to pairs of ARP pulses that switch from $\delta_0 > 0$ in one pulse to $\delta_0 < 0$ in the next pulse [12]. This case, illustrated in Fig. 3(b), shows that changing the nature of the sweep without changing its parameters can increase the efficiency of ARP over a wide range of parameter values. Using $\phi_{\rm rel} = \pi$ effectively changes the sign of Ω_0 so that Ω continues past the north pole as the second sweep begins so that the torque vector evolves continuously and completes its second sweep toward the south pole on the opposite side of the Bloch sphere. The force map for this case is in Fig. 3(d).

As $\phi_{\rm rel}$ is varied smoothly from 0 to π for the up-up sweeps, the region of high-efficiency ARP evolves quickly from the narrow region of Fig. 3(a) to the broader region of Fig. 3(c) even for $\phi_{\rm rel} < \pi/2$, and then stays quite robust in the region $\pi/2 < \phi_{\rm rel} < \pi$. Although such phase shifts could be controlled, in principle, in any real experiment, the region occupied by a sample of atoms always exceeds the wavelength of the light so different atoms experience different values of $\phi_{\rm rel}$.

It is not difficult to imagine how averaging over values of $\phi_{\rm rel}$ between Figs. 3(a) and 3(c) can result in Fig. 3(e) because the regions of efficient ARP simply expand and distort a bit between these two extremes. By contrast, the same variation of $\phi_{\rm rel}$ in Fig. 3(b) causes the narrow pinch near (0, 1.6) at the left edge of Fig. 3(b) to drift toward the right, ending near (1.7, 1.7) in Fig. 3(d). The evolution between the limits shown in Figs. 3(b) and 3(d) is difficult to visualize without access to the several plots between them. They show that this drift leaves a trail of high-efficiency ARP region that is maintained by the wider regions on each side of the pinch. The consequence is that the averages shown in Figs. 3(e) and 3(f) look surprisingly similar [13].

Two important observations about the effect of $\phi_{\rm rel}$ on the forces from ARP emerge from Fig. 3. First, repetitive sweeps in the same directions are the most robust if relative phase in a pulse pair is equal to π. Second, averaging over relative

phase produces results of the maps for optical force that are independent of the sweep directions as shown in the bottom row of Fig. 3.

B. ARP forces on moving atoms

In all of the calculations described here, the atomic velocity will be kept fixed, thus constituting the "dragged atom approach." Including velocity changes slowed down some sample calculations considerably, but did not change the force results in any noticeable way. Therefore, we feel justified in retaining this approximation.

It is clear from Fig. 3 that the ARP force on atoms at rest is close to its maximum value $F_{\rm ARP}/2$ over a large range of experimental parameters. Atomic motion in the "dragged atom approach" assumes that the velocity v along the axis of the counterpropagating ARP pulses is fixed, leading to constant Doppler shifts $\pm kv$. Therefore, it is reasonable to assume that the ARP force will be in the neighborhood of $\sim F_{\rm ARP}/2$ for all atoms, the motion of which leads to Doppler shifts $\pm kv$ that are well below the sweep range $\pm\,\delta_0$.

With moving atoms, a significant change in $\phi_{\rm rel}$ occurs during the flight of an atom if it moves by more than $\lambda/4$ during the interaction time $t_{\rm int}$ that could be estimated based on the velocity range of the ARP force $|kv| < \delta_0$. Choosing $(F_{\rm ARP}/2M)t_{\rm int} = \delta_0/2k$ gives $t_{\rm int} = \pi M\delta_0/\hbar k^2\omega_m$. Avoiding a significant phase shift then requires that the atomic velocity be $< v_r(\omega_m/2\delta_0)$, a speed always less than the recoil velocity $v_r \equiv \hbar k/M$, corresponding to a few μK or less. Thus, the effect of $\phi_{\rm rel}$ can not be neglected, so we must average over the fluctuations it causes.

To present the effect of atomic motion in more detail, we chose two sets of values for $(\delta_0/\omega_m, \Omega_0/\omega_m)$. The first set (2.4, 1.8) is from our previous work [5] and corresponds to part of the narrow region of the maximum ARP force in Fig. 3(e). The velocity dependence in this case is presented in Fig. 4(a) where the force in units of $F_{\rm ARP}$ is plotted versus velocity (plotted in units of δ_0/k, the velocity where the Doppler shift equals the range of the ARP sweep). It shows that the velocity range where the force is half of its maximum value is $|kv| \approx \delta_0/8$. However, this velocity range is expanded dramatically by choosing laser parameters to be (4.19, 3.39) that correspond to the broader region of the maximum ARP force in Fig. 3(e).

One of the most obvious features of Fig. 4 is the multitude of very narrow spikes, especially at higher velocities. These are resonances that occur when the atomic velocity satisfies

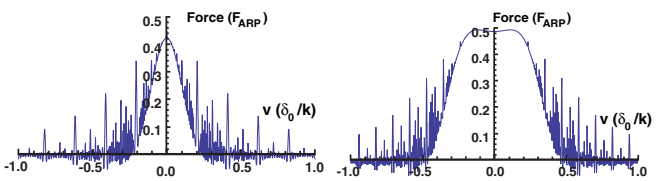

(a) (2.4, 1.8) (b) (4.19, 3.39)

FIG. 4. (Color online) The velocity dependence of the ARP force for various values of the light field parameters given as $(\delta_0/\omega_m, \Omega_0/\omega_m)$ for 12 pulse pairs. These two sets of parameter values were chosen from the white region of Figs. 3(e) and 3(f). Here ϕ_{pp} was fixed at 0, but $\phi_{\rm rel}$ was averaged.

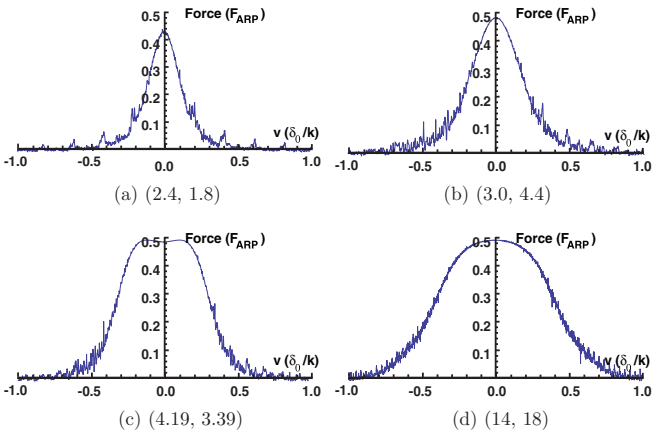

(a) (2.4, 1.8) (b) (3.0, 4.4)
(c) (4.19, 3.39) (d) (14, 18)

FIG. 5. (Color online) Force vs velocity plots with averaging over both $\phi_{\rm rel}$ and ϕ_{pp} for three parameter sets matching those of Fig. 2 of Ref. [5] [parts (a), (b), and (d)] and one [part (c)] corresponding to the wide part of Fig. 3(e).

$v = f\omega_m/4k$, where f = rational fraction, as suggested in Appendix B of Ref. [7], and are not computational artifacts. This velocity condition implies that atoms move by an integer number of half wavelengths during a time of (pulse pair + dead time $= 2 \times 2\pi/\omega_m$) so that atoms experience all pulse pairs with the same value of ϕ_{pp} [8].

In experiments, however, ϕ_{pp} can not be kept fixed. During the interaction time, each atom may experience a range of values of both $\phi_{\rm rel}$ and ϕ_{pp} as discussed above. Therefore, Fig. 5 is based on averages over both phases. For $\phi_{\rm rel}$, we choose 21 evenly spaced phases and then average all results. For ϕ_{pp}, the phase is determined by random numbers at the beginning of each pulse pair, and the calculation is averaged over the 21 values of $\phi_{\rm rel}$. Then, the procedure is repeated 25 times and the averages are averaged.

The velocity dependence of the ARP force is plotted for four sets of parameters in Fig. 5, chosen from our previous work. Each of the four plots in Fig. 5 shows that the height of the spikes is strongly reduced by the averaging over the phases, and three of them show that the velocity range $|kv| \approx 1/4\delta_0$.

IV. THE EFFECTS OF SPONTANEOUS EMISSION

The optical Bloch equations given in Eq. (2) have the inherent capability to allow relaxation, particularly spontaneous emission. Spontaneous emission serves as the origin of the word "rapid" in ARP by requiring that the frequency sweep rate be much larger than the natural decay rate γ as stated in Eq. (1). Otherwise, the concomitant damping reduces the atomic coherence established by the laser light and it precludes complete atomic inversion.

A typical dependence of the force on the ratio of ω_m/γ is shown in Fig. 6 for 12 pulse pairs with $\delta_0 = 4.19\omega_m$ and $\Omega_0 = 3.39\omega_m$. The solid curve is for an atom at rest, while the other three are for atoms with $v = \delta_0/3k$ and different sweep directions. When $\omega_m/\gamma \sim 1$, spontaneous emission returns the atom to the ground state frequently enough that the counterpropagating pulse pairs are inefficient at transferring momentum $2\hbar k$ to the atoms. As ω_m/γ increases, the atom-light coherence is preserved for more pulse pairs, thus, more

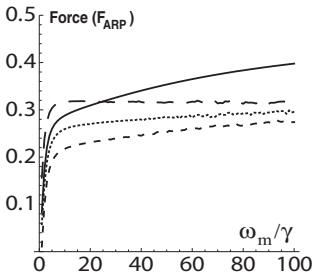

FIG. 6. The ARP force depends on the sweep rate ω_m/γ for $v = 0$ (solid) and on sweep direction for $v = \delta_0/3k$, which is about the velocity where Fig. 5 shows the force has half of its maximum value. The long dashed curve is for the down-down case; the dotted curve is for the up-down or down-up case, and the short dashed curve is for the up-up case. The arrangement of these three curves would be reversed for $v < 0$.

momentum can be transferred from the light field to the atoms before a spontaneous-emission event occurs.

However, satisfying the "rapid" condition (R in ARP) by choosing $\omega_m/\gamma \gg 1$ for a single pulse pair does not eliminate effects of the spontaneous emission on a long sequence of pulses. The possibility of a spontaneous emission to occur before the arrival of the second pulse can have a huge effect because the second pulse would then deliver momentum $\hbar k$ in the wrong direction, resulting in the reversal of the ARP force. Such a force reversal is unlikely to be immediately repeated, thus, many sequential pulses will maintain the force in the wrong direction. On average, the force would vanish. In order to ameliorate this force reversal, we allow a dead time between each pair of pulses. In this case, an atom left in the excited state after the second pulse in a pair has a greater chance to return to the ground state before the arrival of the next pulse pair, effectively restoring the original direction of the force (see Refs. [6,7]).

Figure 7 shows the dependence of the force on the dead time resulting from multiple ARP pulse pairs having $\omega_m/\gamma = 100$. Five choices for the dead time with π/ω_m increments have been considered. For zero dead time (solid curve), the ARP force is reduced to zero after a small number of pulse pairs because of the increased probability of force reversal during a pulse. However, the inclusion of dead time allows for the ARP force to be maintained over many more pulse pairs. The $2\pi/\omega_m$ value for dead time maintains the greatest force over very many pulse pairs, thus justifying its use in this paper.

Choosing $\omega_m/\gamma \gg 1$ and introducing the dead time do not prevent the decrease of ARP force over a long interaction time ($\gg 1/\gamma$). This reduction occurs because the damping in the optical Bloch equations decreases the length of the Bloch vector $|\mathbf{R}|$ from its initial value of unity to a steady-state value less than one. This simply means that the atoms are in a superposition of ground and excited states, and that the coherence has been reduced by the damping associated with spontaneous emission. For the case of $|\mathbf{R}| < 1$, even perfect pulse sequences can not transfer momentum $2\hbar k$ to atoms since the Bloch vector can not reach from pole to pole of the Bloch sphere. This limits the magnitude of momentum transfer by each pulse pair to a steady-state value over long times so that the force scale of Fig. 3 is reduced below $F_{\mathrm{ARP}}/2$, but it does not change the shape.

The velocity dependence of the ARP force with optimal dead time of $2\pi/\omega_m$ in the presence of spontaneous emission is shown in Fig. 8. The plots result from solving the optical Bloch equations for $(\delta_0/\omega_m, \Omega_0/\omega_m) = (4.19, 3.39)$ with phase averaging, and a spontaneous emission rate given by $\omega_m/\gamma = 100$. Two sequences of pulse pairs have been analyzed and are represented by the upper and lower curves for 12 and 60 pulse pairs, respectively. These curves clearly demonstrate that spontaneous emission reduces the magnitude of the force as compared with the plots of Fig. 5. We have found that the steady-state magnitude of the ARP force is reached after 60 pulses, which means that our recent experiments with more than 60 pulse pairs were done in the steady-state regime [6].

The most noticeable effect of spontaneous emission on the ARP force is the unexpected asymmetry with respect to the velocity reversal when consecutive sweeps are in the same direction, as shown in Fig. 8(a). This dependence even survives phase averaging since it is caused by the difference in the time spent by the atom in the excited state $|e\rangle$. Because spontaneous emission tends to reduce the magnitude of the ARP force, the reduction must be larger when the atom spends most of its time

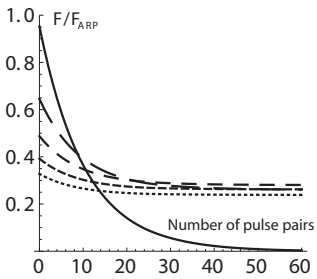

FIG. 7. Force vs number of pulse pairs for various values of the dead time between pulse pairs for atoms at rest. The solid curve is for zero dead time, and the uppermost dashed curve at the left edge is for π/ω_m (longest dashes). Each succeeding dashed curve is for an additional π/ω_m dead time. Although the initial force values are different for a range of dead times, they eventually converge toward $F \approx F_{\mathrm{ARP}}/4$.

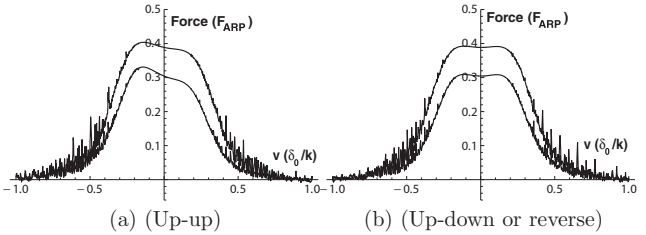

(a) (Up-up) (b) (Up-down or reverse)

FIG. 8. Velocity dependence of the ARP force for two sweep schemes at $(\delta_0/\omega_m, \Omega_0/\omega_m) = (4.19, 3.39)$ as in Fig. 5(c). In part (a), the frequency in both pulses of each pair are swept from red to blue. Sweeps from blue to red produce a mirror image. In part (b), each pulse of a pair has opposite directions for the frequency sweeps, either from red to blue or from blue to red. The results are the same. In both (a) and (b), both ϕ_{rel} and ϕ_{pp} are averaged, just as in Fig. 5. The upper and lower curves are the results for 12 and 60 pulse pairs, respectively.

in $|e\rangle$. This is difficult to see in the the Bloch sphere trajectories because they are complicated and depend strongly on the laser parameters.

In the up-up case, the frequency sweep begins below atomic resonance by δ_0. In the rest frame of an atom in $|g\rangle$ moving with positive velocity in the direction opposite to the **k** vector of the first pulse of a pair, the initial frequency of the field is Doppler shifted upward. The light is initially closer to resonance than δ_0 and the atomic state is driven quickly toward $|e\rangle$ near the beginning of the pulse, and spends the majority of the pulse duration in the upper hemisphere of the Bloch sphere, eventually approaching the north pole. The frequency sweep for the following pulse also begins below resonance but it propagates in the opposite direction so that the atom experiences light with a downward Doppler shift. The initial frequency is further below resonance than δ_0 so that the atom dwells longer in the northern hemisphere of the Bloch sphere before being driven downward toward $|g\rangle$. Therefore, after two pulses with consecutive sweeps in the same direction, an atom moving with positive velocity spends most of its time in $|e\rangle$ (upper hemisphere) and thus experiences a weaker ARP force.

By contrast, if an atom's velocity is negative, then the Doppler shifts are reversed and the atom spends most of its time in $|g\rangle$, resulting in a stronger ARP force. When the two sweeps of a pulse pair have opposite directions, the longer time spent in $|e\rangle$ during one pulse is compensated by the shorter time spent in $|e\rangle$ during the other one, restoring the symmetry with respect to velocity direction, as shown in Fig. 8(b).

V. VELOCITY CAPTURE RANGE

Forces suitable for laser cooling must have significant strength at some velocities and vanish at others. This is the only way for atoms that are initially spread in velocity space to be compressed into the region at the boundary where the force vanishes. Thus, the velocity capture range (v_c) is one of the important parameters for characterizing laser-cooling forces. The utility of such forces depends on their range and strength where they are finite, and their cooling limit is determined by the balance between the steepness of their falloff where they vanish and the heating caused by force fluctuations [1]. The ARP force has strong fluctuations and, thus, is most useful for its large magnitude and capture range.

For the radiative force in the low-intensity limit, $v_c \approx \gamma/k$ and is entirely dependent on the atomic properties. By contrast, the ARP force remains large for velocities where the Doppler shifts are well within the range of the frequency sweep. This means that velocity capture range for the ARP force $v_c \sim \delta_0/k$ can be substantially increased by choosing δ_0 to be larger than γ so that it can be orders of magnitude larger than that of the radiative force. Furthermore, the velocity capture range is not determined only by atomic properties and, in principle, can be applied to different atomic species with optical transitions within the range of the sweep.

The results of our calculations of the velocity capture range for the ARP force in the presence of spontaneous emission and "up-up" sweep sequences are presented in Fig. 9 as a function of δ_0 and Ω_0. The figure confirms that the amplitude of the frequency sweep δ_0 is the most important parameter in defining

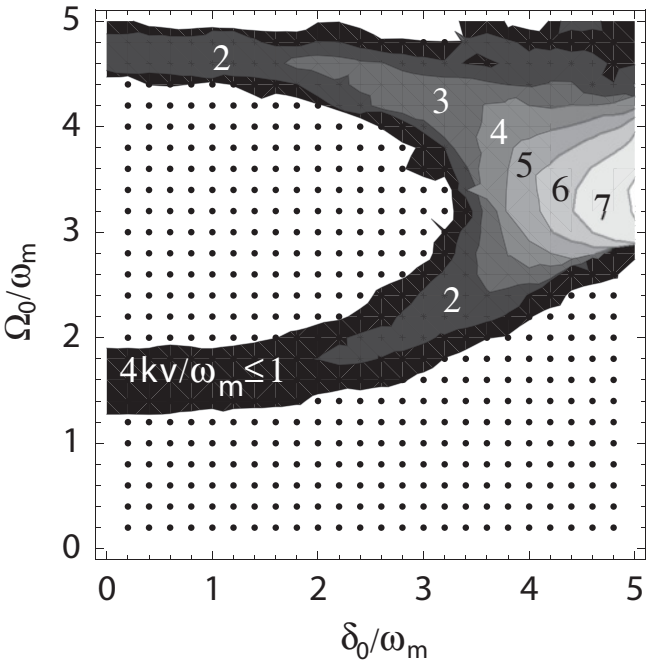

FIG. 9. The shaded area shows the parameter values where the force exceeds $F_{\mathrm{ARP}}/6$, chosen for convenience [in the dotted region the force is always very small as shown in Figs. 3(e) and 3(f)]. Each succeeding lighter area indicates a region where the force exceeds $F_{\mathrm{ARP}}/6$ for the indicated velocity. The velocity increment between regions is $\omega_m/4k$ up to $v = 7\omega_m/4k$ in the white region at the right edge. Since $\delta_0 \sim 4.5\omega_m$ in this region, the velocity is well in excess of $\delta_0/3k$.

v_c. It also shows that the ARP force remains effective (i.e., half of the $v = 0$ value) at velocities up to $\sim \delta_0/3k$. In particular, the ARP force with $\delta_0 = 4.5\,\omega_m$, where $\omega_m = 100\,\gamma$, means that $v_c \sim 150\,\gamma/k$, which is two orders of magnitude larger than the capture range of the radiative force. Such a broad velocity capture range of the ARP force removes the need for Doppler compensation that is required for most beam-slowing schemes.

VI. SUMMARY AND OUTLOOK

We have numerically studied the ARP forces on moving atoms by solving the optical Bloch equations for multiple pulse pairs. Our calculations showed that these forces are much larger than the ordinary radiative force, and depend on the sweep range, peak intensity, and relative phase, but have also found that averaging over the two distinct kinds of phases smoothes the velocity dependence. We present the results of various numbers of pulses, values of atomic velocity, sweep directions, and the effects of spontaneous emission.

We are planning to measure the velocity dependence of the force for different sweep directions to compare with these calculations. To do this, we have developed two independently swept light beams, the center frequencies of which can be shifted to mimic Doppler shifts. Unlike the experiments of Refs. [6,7] that could not vary the sweep direction or center frequency, our implementation can do both. Thus, we can

surpass the simple measurements of the velocity dependence described in Ref. [7] that were done by tilting the laser-beam axes with respect to the atomic-beam direction and were limited by the geometry of the apparatus and compromised by the longitudinal velocity distribution of atoms in the beam.

ACKNOWLEDGMENTS

We acknowledge significant help from Benjamin Glässle in the early stages of this work and Martin Cohen for his experimental help. This work was supported by O.N.R. and Dept. of Education.

[1] H. Metcalf and P. van der Straten, *Laser Cooling and Trapping* (Springer-Verlag, New York, 1999).
[2] L. Allen and J. Eberly, *Optical Resonance and Two-Level Atoms* (Dover, New York, 1987).
[3] P. Berman and V. Malinovsky, *Principles of Laser Spectroscopy and Quantum Optics* (Princeton University Press, Princeton, NJ, 2011).
[4] M. M. T. Loy, Phys. Rev. Lett. **32**, 814 (1974).
[5] T. Lu, X. Miao, and H. Metcalf, Phys. Rev. A **71**, R061405 (2005).
[6] X. Miao, E. Wertz, M. G. Cohen, and H. Metcalf, Phys. Rev. A **75**, 011402 (2007).
[7] X. Miao, Ph.D. thesis, Stony Brook University, 2006.
[8] T. Lu, X. Miao, and H. Metcalf, Phys. Rev. A **75**, 063422 (2007).
[9] R. Feynman, F. Vernon, and R. Hellwarth, J. Appl. Phys. **28**, 49 (1957).
[10] This is the same definition as that in Refs. [5,8] but different from that of Ref. [6].
[11] This can be found at [http://www.math.unifi.it/ brug-nano/BiM/index.html]. It is written especially for stiff, ordinary differential equations and is quite fast and efficient.
[12] In the picture of Ref. [5], it leads to consecutive Bloch sphere rotations in opposite directions for $\phi_{\text{rel}} = 0$.
[13] Appendix B of Ref. [6] shows that the net ARP force averaged over ϕ_{rel} is independent of the ordering or direction of the frequency sweep.